Personal and Ubiquitous Computing manuscript No.
(will be inserted by the editor)

Radio-Frequency-Based Indoor-Localization Techniques for Enhancing Internet-of-Things Applications

Andreas Girgensohn · **Mitesh Patel** · **Jacob T. Biehl**

Received: date / Accepted: date

Abstract An important capability of most smart, *Internet-of-Things-enabled* spaces (e.g., office, home, hospital, factory) is the ability to leverage context of use. Location is a key context element; particularly indoor location. Recent advances in radio ranging technologies, such as Wi-Fi RTT, promise the availability of low-cost, near-ubiquitous time-of-flight-based ranging estimates. In this paper, we build on prior work to enhance this ranging technology's ability to provide useful location estimates. For further improvements, we model user-motion behavior to estimate the user motion state by taking the temporal measurements available from time-of-flight ranging. We select the velocity parameter of a particle-filter-based on this motion state. We demonstrate meaningful improvements in coordinate-based estimation accuracy and substantial increases in room-level estimation accuracy. Furthermore, insights gained in our real-world deployment provides important implications for future Internet-of-Things applications and their supporting technology deployments such as social interaction, workflow management, inventory control, or healthcare information tools.

A. Girgensohn
FX Palo Alto Laboratory, Inc.
3174 Porter Drive
Palo Alto, CA, 94304
E-mail: andreasg@fxpal.com

M. Patel
FX Palo Alto Laboratory, Inc.
3174 Porter Drive
Palo Alto, CA, 94304
E-mail: mitesh@fxpal.com

J. T. Biehl
University of Pittsburgh
School of Computing and Information
135 North Bellefield Avenue
Pittsburgh, PA 15260
E-mail: biehl@pitt.edu

Keywords Indoor Location · Bluetooth Low-Energy · Wi-Fi RTT

1 Introduction

Indoor positioning and tracking are long-standing topics of *IoT* research. As the realization and utility of broader concepts such as smart buildings gain traction, accurate and reliable indoor positioning and tracking techniques have become essential core technologies. Research and industry have proposed many technology approaches to indoor location, including audio [21,35], light [43,48], inertial [36], and magnetic sensing [30] approaches. However, most techniques leverage common radios, such as Wi-Fi and Bluetooth Low Energy (BLE) [5,24,12], due to their ubiquity and low-cost. Recently, standards committees and individual companies have published open protocols that can be easily accessed on commodity mobile devices, such as iPhone or Android smartphones.

The predominant focus and driving metric in indoor positioning research has been accurate coordinate position estimation. Specifically, the goal is the low latency and high accuracy prediction of a device's location as a point on a map. The research community has advanced the state-of-the-art in coordinate positioning, contributing technology algorithms [40,47], evaluations [17], and thought leadership [44]. These efforts have established standards and goals for this research.

While less studied, room-level location estimation is also important to develop and evaluate. Many *IoT* concepts depend on room-level estimation rather than coordinate estimation. Consider the *IoT* home and the simple act of customizing a mobile user interface to control the devices in that room. For this use context to be useful and effective, the interface needs to know with high certainty that the device is in the correct room. In office settings, room estimation provides information about colleagues interactions, supporting social awareness. Similarly, in *IoT* medical environments, accurate room estimation is critical for tracking patient movement and interaction with care providers. Reliable room-level estimation can drive a range of useful applications, including workflow management, inventory control, and patient information tools. Our previous work on workplace communication used room-level location to facilitate awareness among colleagues [7].

Research into new enabling technologies has shown dramatic improvements in coordinate estimation accuracy. For instance, Wi-Fi RTT [18] that uses round-trip time has been shown to achieve ranging accuracy within one to two meters [17]. Despite these advances, there has been little experimentation and validation of these new technologies for accurate room-level location estimation in authentic environments. There is likewise poor understanding of how the mechanisms to improve coordinate location estimation, such as map-based geometric constraints [31], impact room-level estimation accuracy.

For improved accuracy, we utilize ranging information from Wi-Fi RTT sensors to both sense the environment and to detect different motion states of the user such as dwell or walk speed. The motion state is vital for various real-world applications as users will dwell in different spaces in the environment and walk with different speeds depending on their tasks. The dynamic update of the motion state allows our system to better adapt and accommodate for the uncertainty present in the motion behavior of the user.

This paper is an extended version of [6], introducing for the first time our user motion modeling approach for improved accuracy. In this paper, we seek to determine the utility of these emerging technologies. Specifically, we make the following contributions

- Conduct the first evaluation of Wi-Fi time-of-flight to support room-level location. Evaluate the suitability of established estimation techniques, e.g., particle filters [40], to perform room-level estimation with geometric projection.
- Perform a direct comparison to state-of-the-art techniques for room-level location estimation. Compare the efficacy and performance of techniques that use Wi-Fi time-of-flight ranging estimates to those that use Bluetooth Low Energy signal-strength-based ranging estimates (e.g., those provided by common frameworks such as iBeacon[1] or Eddystone[2]).
- Provide a density analysis that correlates Wi-Fi time-of-flight beacon density with estimation accuracy. Also analyze density performance for Bluetooth Low Energy deployments, providing important context for comparison.
- Situate the density performance of Wi-Fi time-of-flight beacon density within the context of Wi-Fi access point density for data coverage. Explore the effect of increased density for indoor location estimation accuracy.
- Model user motion by detecting motion states to improve location accuracy.

2 Related Work

Radio-based ranging combined with multi-lateration or multi-angulation are the most common approaches to indoor location estimation [40,47,23]. The overall estimation accuracy is dependent on the reliability of the radio ranging measurements. Until recently, radio-based ranging precision was only achieved reliably using Ultra-Wide Band (UWB) radios [44]. This changed with the emergence of the Wi-Fi IEEE 802.11-2016 Fine Time Measurement specification [18]. It accurately measures the round-trip time (RTT). From now on, we will refer to this technology as Wi-Fi RTT. Verification has shown that the technique provides reliable indoor-ranging data [17]. In this work, we evaluate and compare the performance and deployment characteristics of these emerging ranging techniques to support highly-accurate room-level estimation while also comparing performance to benchmark approaches.

RF sensors have also been studied to model various user behavior for localization. For example, Iqbal et al. used a deep-learning-based system to classify various user motion states such as move forward, backward, or no movement [19]. Their system was trained with data collected from Wi-Fi sensors. Adib et al. developed a multi-person localization system called WiTrack2.0, that uses the wireless signals reflected off people's bodies [1]. That system is built using an array of directional transmitter and receiver antennas. The time travelled by the signal from the transmitter to receiver after a reflection is used to calculate the distance of the user from the antennas. The distance information is further used to localize user. Apple introduced UWB in the iPhone 11 for improved spatial awareness. As UWB has a bandwidth of at least 500 MHz, one should expect higher accuracy compared to Wi-Fi RTT. At the same time, UWB is blocked by walls such that only line-of-sight measurements are feasible.

Several alternative technology approaches exist to track a device indoors, especially at the room-level. A significant amount of work and commercialization efforts have focused on fingerprinting the signal-strength characteristics of Wi-Fi [5], Bluetooth [24], ZigBee [9], or combination of radio signals [12] to provide accurate room-level localization. Extending radio fingerprints with additional sensor information can further improve the accuracy and robustness

[1] `https://developer.apple.com/ibeacon/`
[2] `https://developers.google.com/beacons/eddystone`

of these predictions [3,26,37,39]. Unlike ranging-based approaches, fingerprinting requires significant training data to properly construct and regularly update a robust classification database. While there are efforts to automate and model this work [4,16], this limitation inhibits large-scale deployments.

Coded light, emitted from a visible-light lamp, is a reliable technique for room-level location. Light-based localization approaches may use the camera or light sensor on a mobile device to detect binary encoded location pattern [43] or leverage polarized light [48]. Advanced light sensors and projected location sequences provide sub-room accuracy [29]. Similarly, audio has also proven effective across a variety of approaches including audio fingerprinting rooms [21,35], proximity beacons,[3] and techniques that leverage microphone/speaker arrays for angle-based 3D geometric localization [11,27]. While effective, the density requirements make these approaches expensive to deploy. Furthermore, their use require the device to have an unobstructed path to the emitted light or audio signal, preventing tracking when a device is in a pocket or improperly oriented. Privacy concerns are also prevalent with audio- and camera-based sensing techniques [25].

User motion modeling using RGB and depth sensor have been explored by robotics and computer vision researchers to develop vision-based localization systems. Kendall et al. proposed an end-to-end deep learning model that learns and predicts the 3D pose of the user using RGB images. Furthermore, Wang et al. used a deep learning model that predicts the motion of the robot using a sequence of images [42]. The overall aim of this system is to estimate ego motion from a sequence of images and not the user's state. Song et al. combined an RGB-D camera and a LiDAR sensor for localization in aerospace missions, service robotics, and intelligent vehicle systems [38]. To distinguish falling from other motion such as sitting, Zhou et al. used vision-based motion classification and ultra-wideband radar [49].

Location approximation performed using inertial and magnetic sensors has been shown effective for classifying among a small number of rooms [30,36]. Traditionally, IMU has been the go-to sensor for modeling various user behavior including motion-related behaviors. Pei et al. utilized the accelerometer and magnetometer signals of an IMU to detect various user states, e.g., walking or standing, and to determine the position of the user [33]. Similarly, De Cillis et al. utilized an IMU sensor to determine the step count and orientation which were further used in their proposed positioning algorithm. Using this approach, the authors claim they achieve better room localization accuracy [13]. Researchers have also developed systems where IMU information is fused with other sensors such as camera images and RF sensors. For example, Lupton and Salah [28] proposed a visual inertial navigation system that fuses IMU information with images. Xu et al. proposed a localization system that utilized IMU-based pedestrian dead reckoning and fused it with photodiode sensors on smartphones to detect illumination changes [46]. Wang et al. fused Wi-Fi signal propagation with IMU sensors using a Kalman Filter (KF) to provide highly accurate localization and tracking. Similarly, Yoon et al. proposed a KF-based system that fused the RSSI from BLE with IMU measurements that are further smoothened using a Rauch-Tung-Striebel smoother. Lastly, in our previous work we utilized an IMU sensor to detect the direction of the user motion and fused it with BLE measurements to perform localization [20].

However, tracking in large spaces, such as office buildings, hospitals, and factories is difficult to scale. More complex systems can leverage radio tomography [45] or wireless signatures from Wi-Fi channel state information [8] to count and identify people in rooms. Other techniques leverage a building's existing electrical system to emit detectable electromagnetic tones that can be detected as location signatures [32]. These emerging technologies show great promise but lack wide-scale evaluation in authentic environments. In contrast, our current work provides an actionable feasibility evaluation of technologies that will soon enter wide-scale adoption and deployment.

3 Estimation Techniques

We look at contemporary approaches to indoor location estimation employing multi-lateration and multi-angulation mechanisms with common communication radios (e.g., Wi-Fi or Bluetooth). These approaches provide two very important advantages. First, they enable devices to be located without additional end-user cost (radios are already available in most modern mobile devices). Second, they do not require significant data collection and data maintenance to deploy (no fingerprinting required, just the location of deployed beacons). Borrowing insights from the robotics community, indoor location estimation researchers have employed signal filtering techniques with great success. Researchers have successfully applied Particle Filter [40], Kalman Filter [47], and Extended Kalman Filter [23] to indoor location estimation.

Many commercially available frameworks provide a proximity-based approach to indoor location. For instance, frameworks such as iBeacon and Eddystone are designed to allow application developers to actuate events when a device is within a specific range of a beacon. Because of their commercial availability, our evaluation also compares the use of these simplified approaches to room-level location. We describe the technical fundamentals for each of these indoor location estimation techniques.

[3] `https://chirp.io`

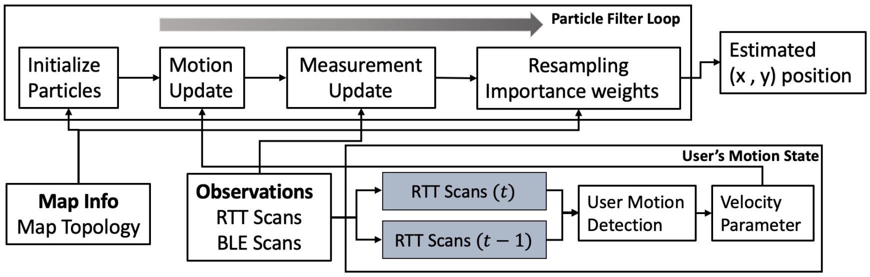

Fig. 1: Overview of our particle-filter-based localization system that utilizes different information (i.e., user motion model, map information) to improve the overall position estimation. The user motion is detected by using the temporal difference between the Wi-Fi RTT scan measurements which is in turn used to control the velocity parameter. The map information is used during the initialization of particles and re-sampling phase.

3.1 Room Estimation using Particle Filter

Filtering techniques utilize ranging and signal-strength observations that are non-linear in nature and the posterior density is multi-modal. A particle filter (PF) is a non-parametric implementation of the Bayes filter and suitable for tracking and localization problems where dealing with global uncertainty is crucial [41]. Our implementation utilizes a Sample Importance Resampling filter embedded with a systematic resampling algorithm. To detect the degeneracy and perform resampling, we compute the effective sample size that corresponds to the reciprocal of the sum of squares of particle weights.

We define our problem with the particle filter paradigm and briefly explain the preliminaries. Let $\mathscr{M} = \{m^{[j]}\}_{j=1}^{n_m}$ be a set of known and fully observable features whose elements, $m^{[j]} \in \mathbb{R}^3$, represent the beacons' location (marked in Figure 2). The receiver (smartphone in our case) can only receive the signal strength or ranging information that are broadcast by the beacons. Let $Z_t \subset \mathbb{R}$ be the set of possible measurements (signal strength or ranging) at time t. The observation consists of an n_s-tuple random variable $(z_t^1, \ldots, z_t^{[n_s]})$ whose elements can take values $z_t^{[k]} \in Z_t$. We denote the position of the receiver up to time t by $x_{0:t} \triangleq \{x_0, \ldots, x_t\}$ where $x_t \in \mathbb{R}^3$. Lastly, we denote the weights of each sample particle as w_t^i which corresponds to the position of user x_t^i.

Given the set of known beacon positions $\mathscr{M}$ and noisy measurements Z_t, the particle filter algorithm recursively operates in two phases: *prediction* and *update*. Each particle is modified according to the existing model, including the addition of random noise in order to simulate the effect of noise on the variable of interest, the receiver position, x_t. Then, each particle weight is re-evaluated based on the latest observations Z_t. The estimation of the posterior density function of the state is given by Equation 1.

$$p(x_t|Z_t) \approx w_t \cdot \delta\left(x_t - x_t^i\right) \tag{1}$$

where x_t^i is the i$^{\text{th}}$ sampling point or particle of the posterior probability and w_t is the weight of the particle and δ is Dirac delta measure [2].

Problem 1 (Positioning)**.** *Let $z_{1:t} \triangleq \{z_1, \ldots, z_t\}$ be a sequence of range measurements from RTT beacons up to time t. Let x_t be a Markov process of initial distribution $p(x_0)$ and transition equation $p(x_t|x_{t-1})$. Given the measurement model $p(z_t|x_t)$, the objective is to estimate recursively in time the posterior distribution $p(x_{0:t}|z_{1:t})$.*

Problem 2 (Motion Model)**.** *Let U_t be the action taken by the user (i.e., walking or being stationary) at time t. Given the motion state of the user, the objective is to dynamically update the velocity parameter sv that updates the state of the particles during the motion-update phase.*

The first problem is formulated as a localization problem that is solved using the PF framework. The second problem is formulated as detecting the discrete user motion states of dwell, slow walk, and normal walk. This motion state is utilized to condition the velocity parameter σ_{sv} of the PF that dynamically changes the velocity at which the particles are displaced. Details of this can be found in Section 3.3. Figure 1 shows the diagram of the architecture and data flow of our system. The PF based localization system initializes the particles randomly over the environment. In case of map availability, the particles are initialized in areas where user will most likely walk (e.g., hallways, rooms). Once initialized, the system goes through an iterative process of motion update and measurement update. In the motion update phase, each particles is randomly displaced using either the constant velocity σ_u, σ_v or σ_{sv} (if the user motion model is used). During the measurement update phase, the weights of the particles are updated based on the distance information received from the Wi-Fi RTT or BLE beacons. Lastly, in order to avoid degeneracy, we use a low variance re-sampling technique to sample new particles and remove old particles with smaller weights.

We make the following assumptions for the RTT beacons used for localization. For simplicity, since the locations of the beacons are known, they are eliminated from the conditional probability terms.

Assumption 1 (Fixed channel bandwidth)**.** *The channel bandwidth for all the RTT beacons is fixed at* 80 *MHz as it gives more accurate distance estimates compared to* 40 *MHz bandwidth.*

This was reported in [17]. Since the bandwidth leads to different ranging behavior (i.e., over- or under-estimating), this assumption guarantees that the sensor behavior is uniform across all the beacons.

Assumption 2 (Known data association)**.** *Each beacon has a unique hardware identifier that is available to the receiver device.*

This is normally the case as the unique MAC-address of each beacon is provided together with the ranging data. Hence, this assumption relaxes the need for data association. Finally, we assume that the only available information to the receiver is the distance estimate.

Assumption 3 (Ranging correction)**.** *At short distances, the RTT beacons provide estimates that may be too short by several meters.*

Through further experimentation we can confirm that short distances are underestimated with an 80 *MHz* wide channel which were in line with the results reported by [17]. To incorporate this error within our system and get a threshold below which the distance estimates needed correction, we performed experiment where data was collected over different distances for different beacons. The threshold value of 5 *m* was derived based on error distribution. Lastly, for error correction, we used linear regression to get the slope and offset values of 0.045 and 2.25 *m*, respectively, that adjust the distances close to the true distances. Equation 2 provides the mathematical model of how the distance estimates are updated. In Tables 1 and 3, the corrected distances are marked with "+Dist" and show noticeable improvements for raw scan error as well as coordinate and room-level localization compared to the corresponding entries without distance correction.

$$d' = \begin{cases} \max(0, 0.45 * d + 2.25\ m) & \text{if } d < 5\ m \\ d & \text{otherwise} \end{cases} \qquad (2)$$

When using signal strength as measurements, as is the case for using Bluetooth Low Energy (BLE) data, we convert the distance between beacons and particles into the signal-strength domain using the path-loss model.[4]

[4] https://en.wikipedia.org/wiki/Log-distance_path_loss_model

3.2 Using Map Information

To model the map geometry in the experiments, we incorporated the map information within our PF framework. The map geometry is incorporated in different stages of the particle filter, i.e., initialization and re-sampling. During initialization, the particles are sampled in areas where the user can visit, e.g., hallways and rooms. During re-sampling, the positions x_t^i of the new particles are conditioned to the map geometry by either snapping them to the nearest navigational edge or moving them from a room's perimeter towards the center of that room [31].

To predict the room location that the smart device user occupies, the estimated coordinates of the particle filter are checked against the boundary of each room. For efficiency, a precomputed grid indexes the room shapes that overlap each grid cell.

3.3 User Motion Model Using RF Sensors

In real-world applications, the motion of a user is unpredictable and highly dependent on the task the user is trying to perform. Hence, user motion cannot be modeled as a constant velocity model (sv) and should be adaptive to account for the dynamic changes in users' motion (Ms).

To elaborate this further, consider the situation of a user performing a targeted task of attending a meeting in a particular conference room. This can be broken down into subtasks, such as the user walking to the conference room from their office, possibly at different speeds, and staying stationary after arriving in the conference room. User states such as dwell and different walking speeds should be incorporated within the PF algorithm for better localization estimates. As shown in Figure 1, to derive the state of the user (e.g., moving or stationary) we iteratively use the difference in the ranging data received from Wi-Fi RTT beacons at time $t-1$ and t. The average of the distances over all the respective beacons is further used to discretize the user's motion state into three categories *dwell, slow walk, normal walk.* This discretized motion state inferred from the RF sensor is further utilized to condition the velocity parameter σ_{sv} which is used to update the state of the particles during the motion update phase. It should be noted that the categories of the discretized motion states can be divided more finely or coarsely based on the problem at hand. Through our experiments we found that in an office space, three categories are sufficient to define a user's motion state. Lastly, in order to overcome singularity issues when deriving a user's motion state, ranging data at times $t-1$ and t has to have at least two common beacons. To incorporate this issue in the motion model, our system will fall back to default value of motion parameters (σ_v and σ_u) listed in Table 2 if this requirement is not met. The conditioning of velocity parameter σ_{sv} which in turn leads to the update of the state of each particle in PF can be represented as follows.

$$p(\hat{x}_t^{[i]}) = \begin{cases} p(x_t^{[i]}) + (\sigma_v, \sigma_a | Ms) \cdot dt + \mathcal{N}(0, \sigma_s^2) & |\cap| \geq 2 \\ \sigma_v, \sigma_a = 0.1 & \text{otherwise} \end{cases} \tag{3}$$

where $p(\hat{x}_t^i)$ is the state of particle i at time t of PF after motion update, sv is the velocity parameter, Ms is the motion state of the user derived from the temporal data available from Wi-Fi RTT beacons, dt is the time difference between current and previous timestamp of when the RTT ranging data was received, $|\cap|$ is number of common beacons at $t-1$ and t, and $\mathcal{N}$ is the Gaussian noise.

3.4 Room Estimation using Closest Beacon

For completeness, we also compared the performance of the PF-based estimation technique against the Closest Beacon (CB) technique. This approach requires at least one beacon in each target room. For each set of scans received during a short interval, the closest beacon is selected and the room containing that beacon is chosen. Due to the noisy characteristics of beacon scans, further smoothing techniques such as a median filter or a majority vote system are needed to achieve better room estimation.

4 Experimental Methodology

We evaluated the performance of our system with respect to room prediction and error of estimated location. We tested our system on a dataset collected locally in a 252 m^2 area inside our office space. We compared the performance of BLE and RTT beacons subsampled to different numbers. Finally, we applied a particle filter system with variations such as map alignment and user motion modelling.

4.1 Data Collection

For the experiments, we used an area of 21 $m \times 12$ m out of a total single floor area of 52 $m \times 44$ m (see Figure 2). The space consists of typical office layout with partitioned rooms and corridors. Each office has furniture such as desks, chairs, book shelves, whiteboard, meeting table, etc. The building construction is typical for contemporary office buildings on the United States' West Coast. From previous experiments, we had BLE beacons deployed in most rooms. For direct comparison of the technologies, the 11 Wi-Fi round-trip time beacons (RTT) were placed in locations that also had a BLE beacon, see Figure 3a.

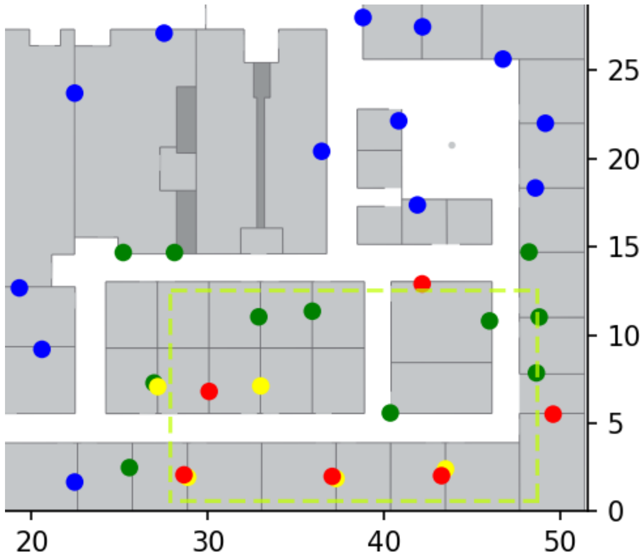

Fig. 2: Beacon placement on the floor plan. Red and yellow locations are shared by BLE and RTT beacons while green and blue locations are only BLE. The dashed line is the bounding box of the ground truth in the experiment.

Figure 2 shows the locations shared by BLE and RTT beacons on the map. Those locations are colored either red or yellow depending on whether they were included in an experiment with sub-sampled beacons. Locations only occupied by BLE beacons are colored green or blue depending on experimental configuration.

The BLE beacons consist of an Electric Imp[5] and a Laird BL600 with a custom case for AC power. The RTT beacons are Compulab WILD Wi-Fi RTT routers [10]. The router is a Linux system with an embedded Intel Atom E3950 and an Intel 8260AC card. From our previous experiments, we found that a 40 MHz wide Wi-Fi channel overestimates distances that are not in direct line-of-sight. Hence, the Wi-Fi options are configured via hostapd.[6] Unfortunately, the country code is locked at 00 such that channel 42 is the only available 80 MHz wide channel. We moved all our organization's Wi-Fi access points (not part of this experiment) away from that channel to avoid interference. The ranging requests use little bandwidth such that using the same channel for all RTT beacons does not cause problems.

To test our hypothesis, we collected data consisting of RTT ranging scans and BLE signal-strength scans along with corresponding ground-truth coordinate locations. For logging RTT scans and BLE signal-strength data, we developed a data logger application for Android and iOS devices, respectively. For logging RTT scan data, we

[5] https://www.electricimp.com/

[6] https://en.wikipedia.org/wiki/Hostapd

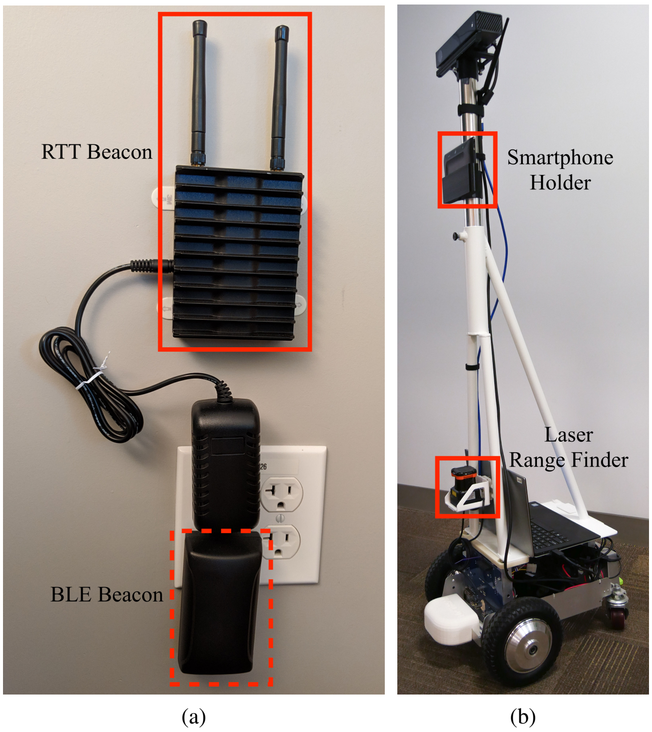

Fig. 3: A sample of placement of RTT and BLE beacon is shown in (a). Robot platform used for data collection is shown in (b).

utilized an Android Pixel 3[7] that supports Wi-Fi RTT [18]. It should be noted that a limitation in Android 9.0 only allows the device to range with 10 RTT beacons at a given time. Our data collection application scans for available Wi-Fi beacons every 30 seconds and uses the 10 strongest beacons. In this way, the application is usually ranging on the 10 closest RTT beacons. BLE signal-strength data was collected on an iPhone X.[8] We used an iOS device because Apple's Bluetooth implementation provides more reliable and frequent BLE advertisement data.

For ground-truth data, we utilized a Magni Robot platform.[9] The robot (shown in Figure 3b) is equipped with a Hokuyo laser range finder[10] that has a range of 30 m and a scanning angle of 270°. We generated ground-truth pose estimation from the range finder data using the hector mapping algorithm [22] developed for Robot Operating System (ROS) [34]. Due to the long range of the laser sensor, the hector mapping was able to generate ground truth with accuracy in a range of centimeters. Furthermore, the Android device running our data-logger app was deployed on the robot.

Table 1: Errors in meters of beacon scans against ground-truth distances. BLE signal strength is converted with the path-loss model.

Beacon Type	Beacon Count	RMSE (m)
BLE	6	4.625
BLE	11	4.508
BLE	22	4.690
BLE	56	5.372
RTT	6	2.642
RTT-Dist	6	2.254
RTT	11	2.564
RTT-Dist	11	2.150

Care was taken to synchronize clocks on all devices before data collection by running the network time protocol against servers synchronized by atomic clocks.

We collected both RTT ranging scans and BLE signal-strength data and grouped them into 5 Hz groups. For multiple scans of the same beacon in the same group, the median was used. Grouped data were aligned to ground-truth coordinate locations. We conducted two runs of 18.7 and 16.7 minutes, respectively, and averaged the accuracy of the runs. It should be noted that data was collected on a working day such that office personnel interfered with radio signals as expected. For RTT, negative scan results were set to zero even without distance adjustment. For BLE, the path-loss model with an exponent of 2.25 was used to compute distances from signal strength. We determined the path-loss exponent in prior work [31] in the same office environment by linear regression of signal strength against the ground truth distance. Table 1 shows the root mean square error (RMSE) comparing the ranging distance estimates (not coordinate location estimates) against the ground truth distance. "RTT-Dist" indicates the distance correction of Equation 2. As the results show, variation in density does not meaningfully impact anchor-device ranging accuracy for either technology.

We sub-sampled both the RTT anchors and BLE beacons to determine the effects of different densities. For 6 Wi-Fi and BLE beacons, we selected every other room (red in Figure 2). As we collected the data for 11 RTT beacons and the Android RTT framework only allows ranging on up to 10 beacons at a time, one beacon may have been occasionally excluded. For BLE beacons, we additionally selected a total of 22 beacons that were placed within three meters of the ground-truth bounding box (green in Figure 2) and all 56 beacons (blue). With six beacons, there is one beacon per 42 m^2. That is still noticeably denser than our data access Wi-Fi access points with one access point per 229 m^2.

[7] https://www.android.com/phones/google-pixel-3/
[8] https://www.apple.com/shop/buy-iphone/iphone-10
[9] http://ubiquityrobotics.com/magni.html
[10] https://www.hokuyo-aut.jp/search/single.php?serial=169

Table 2: Parameters used in the experiments

Parameter	Symbol	Value
− **Compared SIR particle filter variants:**		
Motion Model	PF+MM	-
Map Information	PF+MAP	-
Motion Model and Map	PF+MM+MAP	-
Distance correction (RTT)	PF+Dist	-
− **Particle filter Parameter:**		
Measurement std. dev. (BLE)	σ_n	6.85 *dB*
Measurement std. dev. (RTT)	σ_n	1.65 *m*
Number of particles	n_p	300
Resampling threshold	n_{thr}	0.83
− **Motion model:**		
Default motion acceleration std. dev.	σ_v	0.1 m/s^2
Default motion position std. dev.	σ_u	0.1 m
Velocity sampling parameter	σ_{sv}	user state
User states derived from RF sensor	dwell mode slow walk normal walk	*Ms*
− **Wi-Fi RTT Beacon Parameters**:		
Channel Bandwidth	–	80 *Mhz*
Broadcasting Frequency	–	5 *Hz*
− **BLE Parameters:**		
Unit power at 1*m* (iBeacon protocol)	a_X	-60 *dB*
Transmission power	–	+4 *dBm*
Min signal-strength cut-off	–	-95 *dB*
Broadcasting frequency	–	10 *Hz*

5 Experimental Results

We used two different approaches for predicting dwell in a room. First, we selected the room containing the closest beacon. Second, we used a particle filter to estimate the coordinate-location and checked for containment in one of the room polygons. To account for the non-deterministic nature of the particle filter technique, we evaluated the results from 100 random runs on the two datasets. Table 2 summarizes the different parameters used in our experiments. Table 3 summarizes measures collected, including root mean square error (RMSE) for location estimation, the means and standard deviations of recall and precision from the 100 runs, and the F_1 scores (the harmonic means of those mean precision and recall). “MAP” indicates the incorporation of map information within the PF framework, whereas “MM” indicates the incorporation of motion model information with the PF framework. The closest beacon technique does not involve any non-deterministic calculation and hence does not have any standard deviation. To understand the impact of map geometry, motion model and corrected RTT ranging scans, we compared the effects of each each component with a baseline model where none of this information was used.

The main accuracy measures used are recall and precision of predicting one of the 11 rooms. Because we do not care about other rooms or hallways, those are combined into one negative class that is excluded from the accuracy measures other than false positives for the 11 rooms. In this context, true positives are correct predictions of being in a room, false positives are predictions for a room while being elsewhere, and false negatives are missed predictions for a room while being there. Recall is true positives divided by the sum of true positives and false negatives. Precision is true positives divided by the sum of true and false positives.

5.1 Room Prediction as the Closest Beacon

We estimated the closest beacon with a strongest-beacon approach using a sliding 9-second window to count the BLE beacons with the highest signal strength. The room containing the beacon with the majority vote in that window was picked. If a beacon outside the target rooms had the majority vote, no room was picked. We selected the 9-second window because it produced the best results from the data to determine how well this approach can work. We adapted the approach to RTT ranging by selecting the shortest reported distance instead of the highest signal strength.

Before settling on this strongest signal beacon approach, we used a different approach to smooth out the noise of scans. In the same 9-second window, we selected the median signal-strength value for each beacon. The beacon with the highest median value was selected. However, this produced poorer results for room prediction with 82.1% recall and 74.4% precision.

The strongest signal beacon approach with majority vote provides 91.3% recall and 72.8% precision with 11 and more beacons (see Table 3). The corresponding F_1 score is 1.32 percentage points lower than that for the particle filter with 11 BLE beacons.

The shortest RTT distance, with majority vote performance, is worse with 85.7% recall and 68.5% precision. When using median values of RTT distances, the results were almost identical. The lower RTT performance can be explained by the fact that RTT ranging is not modified by walls. Therefore, the anchor on the other side of the wall is more likely to be seen as the closest one. Walls have a stronger affect on BLE signal strength than on Wi-Fi RTT such that BLE beacons in the same room are favored.

5.2 Room Prediction with Particle Filter

The particle filter provides an estimate for the coordinate location using RTT ranging or BLE signal-strength data. This

Table 3: Comparison of the results of indoor localization averaged over the datasets for both coordinate and room level with and without incorporating our proposed motion model. We also compared the performance of the system when map information is incorporated with the approach described in [31]. The results are averaged over 100 runs; mean ± standard deviation. The room-level accuracy is presented in terms of precision, recall and F_1 score.

Type	Count	Technique	Coordinate Localization		Room-level Localization		
			RMSE (m)	90^{th} % CDF (m)	Recall	Precision	F_1
BLE	6	PF	2.078 ± 0.176	3.08	72.67% ± 4.15%	74.47% ± 3.22%	73.50%
BLE	6	PF+MM	2.045 ± 0.163	2.98	73.83% ± 3.32%	75.08% ± 2.67%	74.39%
BLE	6	PF+MAP	2.043 ± 0.199	3.03	73.06% ± 6.75%	76.39% ± 2.46%	74.61%
BLE	6	PF+MM+MAP	2.048 ± 0.197	3.08	73.11% ± 6.72%	76.31% ± 2.37%	74.59%
BLE	11	PF	1.670 ± 0.056	2.47	81.87% ± 3.65%	77.82% ± 2.68%	79.78%
BLE	11	PF+MM	1.629 ± 0.053	2.42	84.42% ± 2.63%	80.31% ± 2.61%	82.30%
BLE	11	PF+MAP	1.633 ± 0.053	2.47	81.95% ± 2.00%	79.36% ± 2.88%	80.62%
BLE	11	PF+MM+MAP	1.617 ± 0.050	2.47	83.11% ± 1.82%	80.26% ± 2.30%	81.65%
BLE	22	PF	1.534 ± 0.039	2.37	86.12% ± 2.10%	86.36% ± 1.60%	86.23%
BLE	22	PF+MM	1.521 ± 0.035	2.37	87.06% ± 1.88%	87.71% ± 1.54%	87.37%
BLE	22	PF+MAP	1.516 ± 0.039	2.42	87.50% ± 2.26%	89.08% ± 0.75%	88.27%
BLE	22	PF+MM+MAP	**1.513 ± 0.041**	2.37	**87.77%** ± 2.07%	**89.38%** ± 0.63%	88.56%
BLE	56	PF	1.600 ± 0.035	2.47	84.88% ± 2.67%	85.19% ± 2.01%	85.03%
BLE	56	PF+MM	1.589 ± 0.026	2.47	86.05% ± 2.23%	86.60% ± 1.74%	86.31%
BLE	56	PF+MAP	1.586 ± 0.023	2.47	87.28% ± 1.97%	88.31% ± 0.99%	87.78%
BLE	56	PF+MM+MAP	1.583 ± 0.024	2.47	87.64% ± 1.92%	88.77% ± 0.72%	88.19%
RTT	6	PF	1.722 ± 0.042	2.82	79.75% ± 2.38%	90.12% ± 2.23%	84.61%
RTT	6	PF+MM	1.693 ± 0.040	2.97	80.21% ± 2.43%	90.82% ± 1.75%	85.19%
RTT	6	PF+MAP	1.690 ± 0.039	2.82	80.59% ± 3.22%	91.71% ± 1.61%	85.78%
RTT	6	PF+MM+MAP	1.683 ± 0.039	2.82	80.24% ± 2.80%	91.75% ± 1.21%	85.60%
RTT	6	PF+Dist	1.629 ± 0.022	2.52	84.30% ± 1.03%	92.48% ± 1.79%	88.19%
RTT	6	PF+MM+Dist	1.595 ± 0.014	2.52	84.74% ± 0.71%	93.21% ± 1.66%	88.77%
RTT	6	PF+MAP+Dist	1.603 ± 0.013	2.57	84.30% ± 1.65%	94.63% ± 1.81%	89.16%
RTT	6	PF+MM+MAP+Dist	1.591 ± 0.007	2.52	84.41% ± 0.92%	94.49% ± 1.33%	89.17%
RTT	11	PF	1.412 ± 0.113	2.07	87.18% ± 0.98%	93.62% ± 2.31%	90.28%
RTT	11	PF+MM	1.394 ± 0.118	2.07	87.43% ± 0.99%	94.23% ± 2.29%	90.70%
RTT	11	PF+MAP	1.400 ± 0.117	2.07	86.96% ± 0.76%	94.56% ± 1.86%	90.60%
RTT	11	PF+MM+MAP	1.397 ± 0.115	2.07	87.04% ± 0.87%	94.76% ± 1.95%	90.73%
RTT	11	PF+Dist	1.302 ± 0.096	1.97	90.41% ± 1.51%	96.87% ± 1.05%	93.52%
RTT	11	PF+MM+Dist	1.268 ± 0.100	**1.91**	**90.78%** ± 1.60%	97.51% ± 1.03%	**94.01%**
RTT	11	PF+MAP+Dist	1.272 ± 0.080	1.97	89.94% ± 1.74%	98.10% ± 0.81%	93.82%
RTT	11	PF+MM+MAP+Dist	**1.267 ± 0.085**	1.97	90.00% ± 1.66%	**98.11%** ± 0.82%	93.86%
BLE	11	Closest Beacon	-	-	91.28%	72.77%	80.98%
RTT	11	Closest Beacon	-	-	85.70%	68.46%	76.11%

location is checked for containment in a room polygon. In all experiments the number of particles were fixed to 300. In order to accommodate for the non-deterministic nature of the particle filter, we evaluated the results from 100 independent runs on both datasets. Details of different parameters used in our experiments are listed in Table 2.

With 11 beacons deployed in an area of 252 m^2, there is one beacon per 23 m^2; a high density compared to normal Wi-Fi access point deployments. To understand the effects of the different densities of RTT beacons on overall accuracy, we performed two different experiments. The first experiment utilized data from all 11 RTT beacons whereas the second experiment sub-sampled the Wi-Fi RTT beacons to select a beacon in every other room (red in Figure 2). One beacon may have been occasionally excluded in our dataset when testing the sub-sampled case because the Android RTT framework only ranges on up to 10 beacons at a time.

Each strategy was tested using either the MM or MAP information or a combination of both. The tests were compared to baseline results where MM or MAP information was not used. The performance of room-level localization accuracy was then tested by imposing its estimate onto the floor plan.

Table 3 shows precision, recall, and F_1 score for using different variants of PF with all beacons and with a reduced number of beacons for both BLE and Wi-Fi RTT beacons. With all beacons, there is no improvement for the F_1 score. Interestingly, we see an improvement of 1.64 percentage point using the motion model in the F_1 score with reduced number of beacons for RTT case.

Figure 4 shows a comparison of performance between the baseline (PF+Dist) and either the motion model (PF+MM+Dist) or the map information (PF+MAP+Dist) for the reduced number of RTT beacons. Results are paired by the order of the random runs. One can see that the

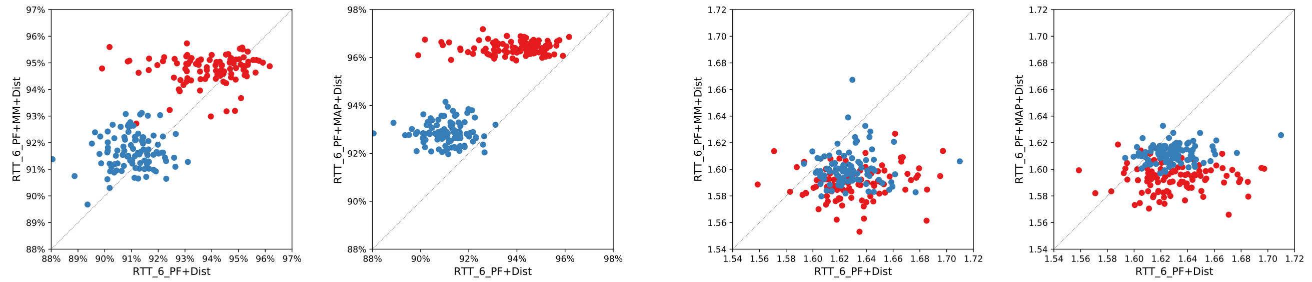

Precision RMSE (m)

Fig. 4: Results for 6 RTT beacons paired by order of the random runs. Color indicates the dataset.

precision of room level prediction forms clusters for the two datasets. The motion model and map information have a superior room precision in 73% and 99% of the runs, respectively. They have a superior RMSE in 93% and 88% of the runs, respectively. This confirms our hypotheses that the motion model performs well for reducing the location error and that the map information improves the accuracy of the room prediction. Both approaches improve both measures compared to the baseline.

Figure 5 shows precision and recall for room predictions for RTT and BLE with different beacon counts. The F_1 score is 11.71 percentage points better for RTT than BLE with 11 beacons and 14.56 percentage points better with 6 beacons (see Table 3). 11 RTT anchors still have an F_1 score of 5.45 percentage points higher than 22 BLE beacons. For 56 BLE beacons, the accuracy is 0.37 percentage points worse than with 22 beacons, likely indicating that farther BLE beacons add noise.

5.3 Error of Particle Filter Location

We use the root mean square error (RMSE) to compare particle filter estimates to the ground truth for both technologies. RMSE, rather than ranging distance error or error ratio, fairly compares the performance of the two technologies. The average RMSE over 100 independent particle filter runs for both datasets combined with all 11 RTT beacons is 1.268 m using our motion model (PF+MM+Dist). It is 1.302 m without the motion model (PF+Dist). When testing with 6 sub-sampled beacons, the RMSE is 1.595 m with the motion model (PF+MM+Dist) and 1.629 m without the motion model (PF+Dist). There is an improvement in the overall RMSE accuracy of 0.034 m both with all beacons and the reduced set.

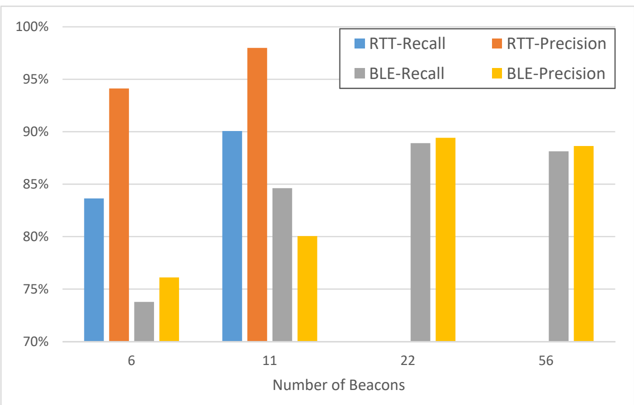

Fig. 5: Accuracy of room prediction for RTT and BLE for different beacon counts.

These results substantiate the hypothesis that by better modeling user motion, the PF is able to update the particles to better align to the motion state of the user. Furthermore, using map information with 6 RTT beacons shows similar improvement of 0.026 m compared to baseline (PF+Dist); especially when the number of beacons and/or measurements in the environment is sparse. The summary of the average of both the datasets for all experiments over 100 independent runs is listed in Table 3.

To differentiate between the noise in the datasets and the degeneracy due to PF, we plot the RMSE for each configuration of PF with both RTT and BLE beacons in Figure 6. The RMSE follows the same trend, i.e., PF performs better when either motion model or map or combination of both is used with all beacons and with sub-sampled beacons.

For completeness, we compared the performance of different variants of PF using Cumulative Distribution Funtion (CDF). The empirical CDF is an unbiased estimate of the population CDF and is a consistent estimator of the true CDF. Using the evaluation method from the EvALL competition [14], the average error for both datasets at the 90^{th} percentile is around 1.91 m for the motion-model-based system (PF+MM+Dist) and 1.97 m without motion model (PF+Dist).

As with the room prediction, BLE performance improves with more beacons and drops when beacons from the other side of the building are included. Table 3 shows the results for different beacon counts. For the same number of beacons, RTT on average performs about 0.4m better

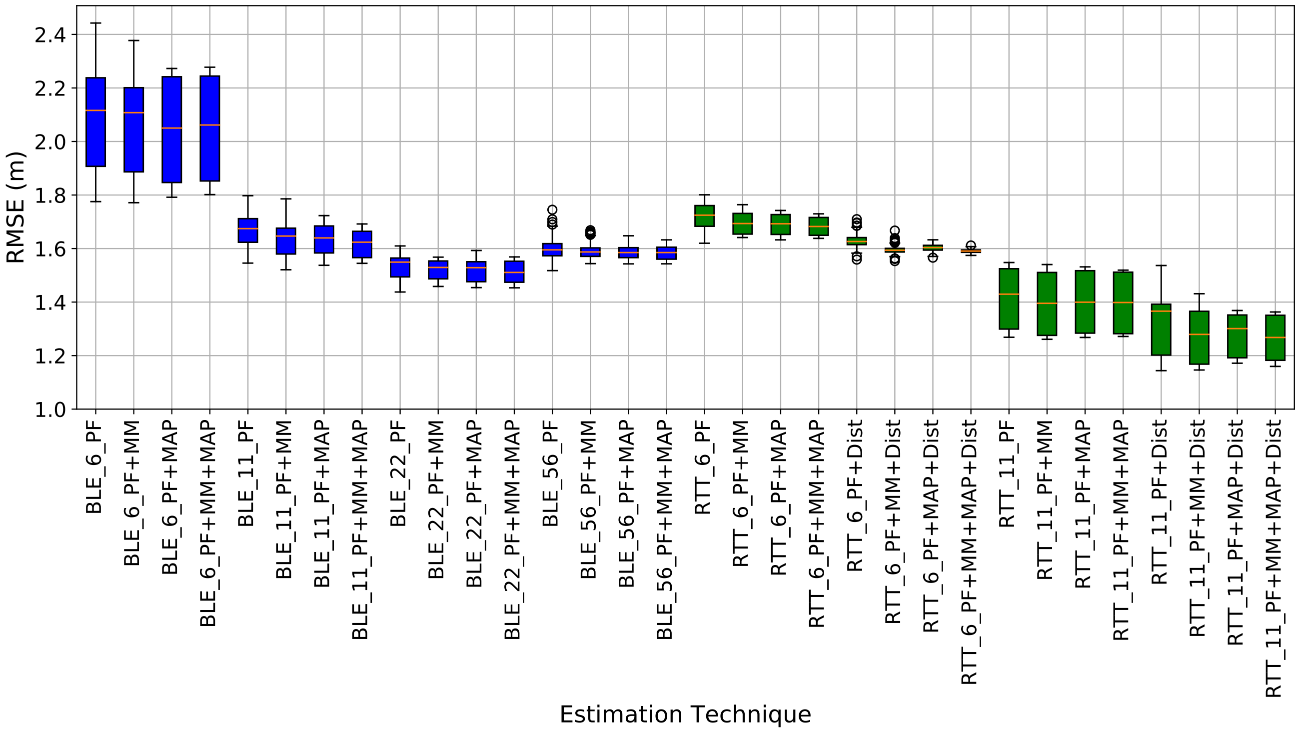

Fig. 6: Coordinate positioning results from 100 independent particle filter runs using different variants for BLE and RTT sensor.

with half as many beacons. When animating particles on the floor plan, RTT particles form a tighter cloud, indicating less noisy data. Figure 8 depicts that the RTT estimates (a, b) follow the ground truth better. However, there are some systematic errors, such as the deviation in the bottom-right room, that do not affect room-level predictions. In comparison, the BLE estimates (c, d, e, f) are less closely aligned with the ground truth.

In Table 3, we show the effects of MAP and Dist for BLE and RTT results. For both BLE and RTT, MAP improves RMSE around 0.03m and room dwell precision around 2 percentage points. Recall remains about the same. Correction of short RTT distances improves RMSE by 0.11m and room dwell accuracy by 3.2 percentage points (see Figure 7).

6 Discussion

The results of this verification experiment provide several interesting implications. Most important, the experiment provides evidential support that use of Wi-Fi RTT [18] distance measurements, though still noisy (e.g., RMSE of 2.15 m), improve the state-of-the-art indoor location estimation accuracy. As shown in our evaluation, Wi-Fi RTT-based location estimations using the same beacon locations achieve 21.6% improvement in RMSE in coordinate location estimation. More important to the focus of this work, the experiment also found a meaningful 6.6 percentage-point improvement in F_1 score room-level location estimation, when comparing high-density deployments of both technologies. When comparing equal densities, RTT-location estimations outperform with a tremendous 11.7 percentage-point difference in F_1 score. The following subsections elaborate our understanding and impacts of different factors such as RF sensor, beacons density, algorithm, room geometry, and modeling motion behavior and conclude with the limitation of our experiments.

6.1 RF Sensor Comparison

The high precision statistics in the RTT-based room-level estimate is notable. These statistics signify that when an estimate is made to be in a particular room, that estimate is 98.1% correct. High precision marks an important turning point in the potential applications that can be powered by indoor location technologies. Many of the applications described in the introduction, especially those targeted for enterprise and healthcare domains, require a high degree of precision in the location estimation that has not been achievable outside high-cost technologies. For example, workflow tools that track health care staff may leverage

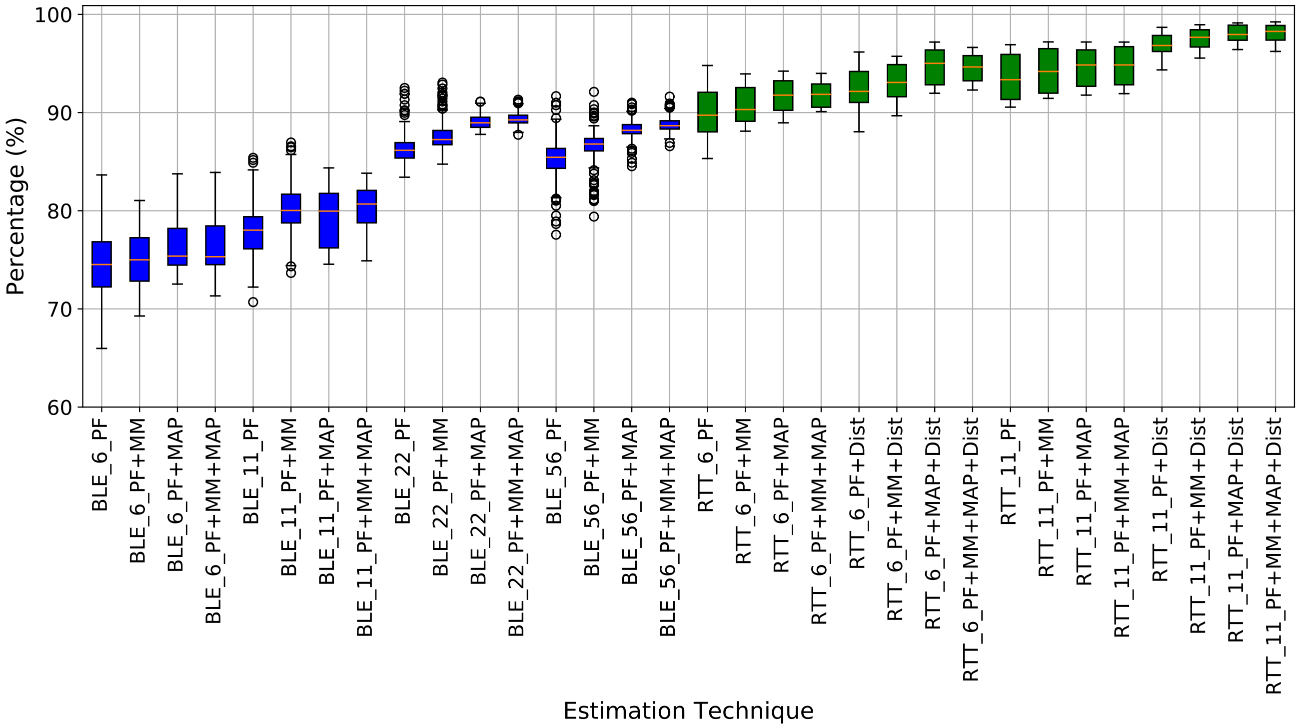

Fig. 7: Precision for room level classification from 100 independent particle filter runs using different variants for BLE and RTT sensor.

location-derived information such as patient co-location, expert co-location, and equipment used. For these workflow statistics to matter, the estimates of where those people and devices are located need to be highly reliable at the room-level.

The performance of our proposed motion model was tested with BLE data collected along the same trajectory. For BLE, the RSSI signal is used as measurement. We used the probabilistic sensor model as specified in [31]. The average RMSE for both the dataset over 100 independent runs of PF for all the beacons is 1.268 *m* using our proposed motion model and 1.302 *m* without the motion model. For the reduced number of beacons, the RMSE is 1.629 *m* and 1.595 *m* with and without the motion model. Our motion-model-based localization system helps less with BLE RSSI measurements with 1.521 *m* and 1.534 *m*, respectively, because those are noisy in nature and hence cannot accurately capture user motion. Similar results are achieved when using Map information for both BLE and RTT sensor. Detailed comparison of each experiment is listed in Table 3.

6.2 Effects of Beacon Density

Beacon density plays an important role in the accuracy of location estimates that is quantified by the results listed in Table 3. Our motion model provides larger improvements for both coordinate and room-level accuracy when there are fewer number of beacons in the environment. This is very important especially for real-world applications because the number of beacons is an important criteria for deploying beacon-based technology (Wi-Fi RTT or BLE).

Another important finding of our experiment is confirmation and quantification of the important role beacon density still plays in driving indoor location accuracy. As our results show, accuracy across coordinate and all room-level location estimations goes down as density drops. In the case of BLE, the drop is understood to be effects of ranging on the long tail of the signal strength. In the case of RTT, the results indicate that multi-path is still a significant design issue for indoor time-of-flight ranging approaches. The implication to developers of indoor location-driven applications is that density, and the direct derivative of cost, will need to be matched based on application needs. For instance, tracking with high accuracy within the individual office will require a heavier deployment than tracking in larger, more open environment such as stores and shopping malls.

Furthermore, while the results show that the overall density of RTT beacons is much lower compared to existing BLE approaches (e.g., 6 compared to 22 beacons for similar accuracy, respectively), the density required for reasonable accuracy is still higher than the typical Wi-Fi access

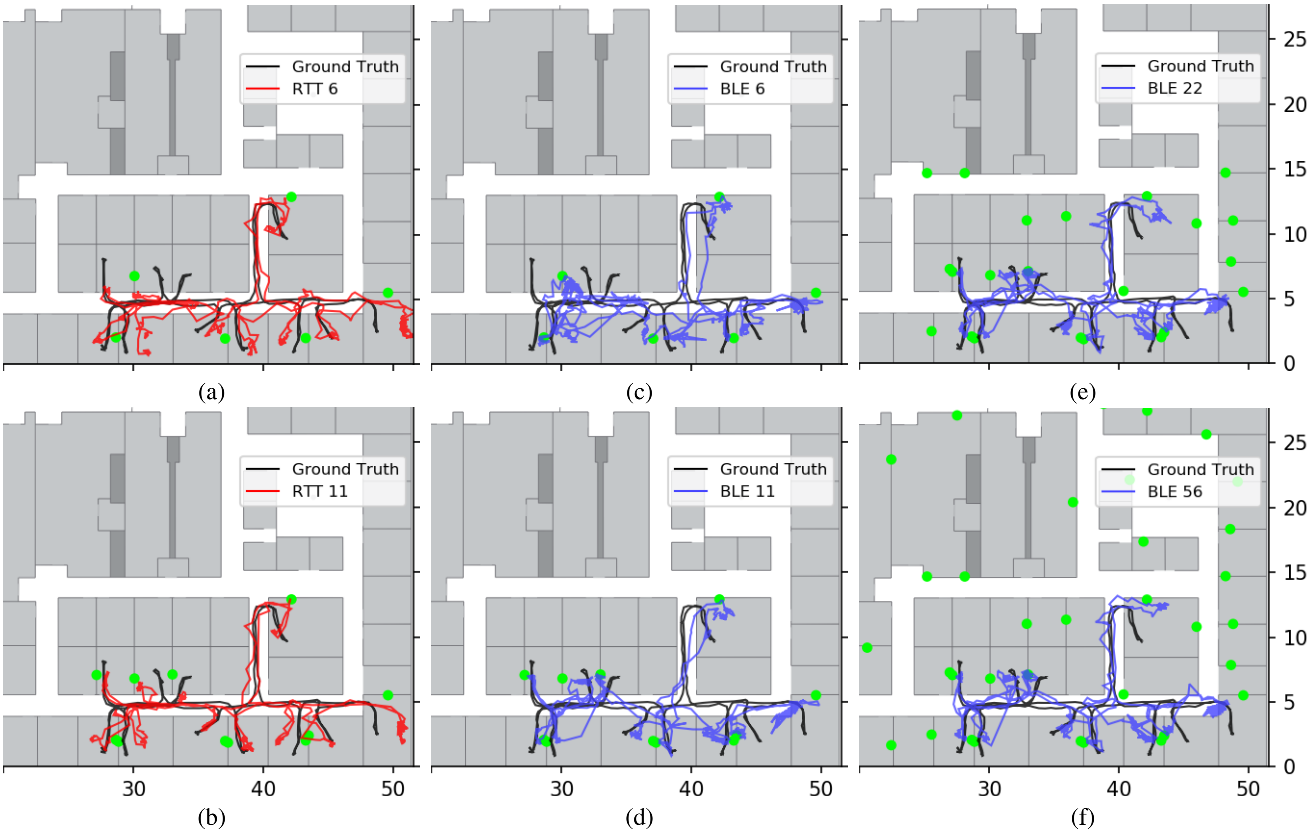

Fig. 8: RTT (red) and BLE (blue) estimates sub-sampled at 1 Hz plotted against the ground truth (black). Beacon counts (light green) indicated in the legends influence the accuracy.

point density. For instance, in the environment studied, the density for Wi-Fi access points is one per 229 m^2. Six beacons in the experiment area correspond to one per 42 m^2, 5.5 times more. Given this difference, it is unlikely that usable indoor location will come for "free" as access points are upgraded to current standards. As Wi-Fi, and even 5G technologies evolve, access point count requirements could decrease. Absent such evolution, density and cost remain an important research criteria for location-tracking capable network design and development.

6.3 Algorithm Comparison

Our experiments also compared the performance of the closest beacon technique (CB) with the more sophisticated particle filter technique (PF). As listed in Table 3, the PF technique for BLE when used with map geometry (PF+MAP) provides a precision improvement of 16.3 percentage points compared to the CB technique. The PF technique for RTT with map geometry and distance adjustment (PF+MAP+Dist) achieves a precision improvement of 29.6 percentage points over CB. This reinforces the fact that PF-based estimation technique are well equipped to compensate for noise inherent in sensor data.

6.4 Impact of Utilizing Map Geometry

Experiments using the map geometry also provided deeper understanding of the improvement on overall performance of PF on both room-level and coordinate localization. Using the map geometry (denoted by PF+MAP for BLE and PF+MAP+Dist for RTT), we found that the precision of predicting the correct room improved by 1.23 percentage points for RTT beacons whereas the same improved by 1.54 percentage points for BLE beacons when compared with results not using the map geometry using 11 beacons. These results show that PF provides better performance if the user behavior is better modeled within the PF framework (e.g., the user will always walk in hallways and enter rooms through doors and not walls).

To study the impact of fusing our proposed motion model with available map information, we used the technique proposed in our previous work [31]. We used map information during different stages of the particle filter. In general, the map information is used to constrain the motion of the particles by aligning them to the paths taken by users (i.e., users will enter rooms through doors and will walk in hallways). As shown in Table 3, the coordinate localization does not provide any improvement when map information and motion model are used as compared to the localization system using only the motion model. This substantiates that our proposed motion model provides at-par localization estimation for situations where map information is not available.

6.5 Modeling User Motion Behavior

Our experiments on modeling different user motion states shows reasonable improvement in the overall prediction accuracy for both room-level prediction and coordinate localization when compared with baseline PF. This is especially observed when fewer beacons are used. For both BLE and RTT, the RMSE accuracy improves by 0.03 *m* over baseline PF for the case of 6 beacons. Similarly, the room level precision is improved by 0.61% for BLE and 1.13% for RTT beacons. At a higher level, by better modeling the users' motion behavior within the PF framework helps align particles to the actual motion of the user (e.g., dwell at a single location, walking very slowly) and hence leads to better performance.

6.6 Multipath Effects BLE vs RTT

Our experiment also found an interesting result with the closest beacon approach for room-level location estimation. This technique has a meaningfully lower accuracy with RTT beacons, despite the beacons themselves being placed in the same positions for all experiments. This illustrates an important difference between using signal strength and time-of-flight ranging techniques. The BLE signals are likely attenuated as they travel through walls from adjacent rooms, resulting in lower signal-strength measurements. This will benefit the signal-strength measurement for the current room as it will not be attenuated in this way. Conversely, the time-of-flight measurements are not meaningfully impacted by attenuation through a wall and thus the resulting closest beacon estimates are not influenced by the natural barriers.

6.7 Limitations

While our experiments provided many insights, there are also limitations in our work. We examined the impact of different beacon densities but our results are based on a single deployment in a single building. Additional examination across beacon placement locations as well as in buildings with different construction materials would further support the mission of this work. It should also be understood that at the time of this experiment and writing, these new standards are just emerging. It is likely that over time the accuracy and reliability of the underlying ranging estimates will improve. Despite these limitations, we believe the discussion above still offers many fundamental insights into the use and utility of these technologies moving forward.

The primary limitation of the motion modeling is the way the dataset was collected with an Android device mounted on a robot. The speed of the robot is capped at 1.0 m/s such that there are insufficient samples for motion behaviors such as fast walk. Hence, we only see a modest improvement in both coordinate and room-level localization.

7 Conclusion

In this paper, we presented techniques for accurate room-level localization. Those techniques can support uses such as social awareness, workflow management, inventory control, and patient information tools. This paper makes several contributions to the *IoT* research community. We provided understanding on the performance of radio frequency sensors, i.e., Bluetooth signal strength and Wi-Fi time-of-flight, used for room-level localization. We compared a closest beacon simplistic localization technique with more sophisticated particle filter techniques. The performance of the particle filter based technique could be improved by incorporating map geometry. A novel technique was presented for modeling user motion behavior using ranging measurements from Wi-Fi RTT sensors deployed in a given environment. Our system utilizes the temporal difference between the ranging measurements to determine the motion state of the user. The detected motion state is utilized by the particle-filter based localization system for estimating the user's location.

Our experiments provided a detailed analysis of the impact of various parameters (e.g., beacon density and map geometry) that affect localization accuracy. Lastly, we provided insights to the research community and to large scale commercial application developers about various implications that needs to be kept in mind when providing large scale indoor location estimation solutions that can be used to power a variety of location based application such as workflow management, social interaction, inventory control and/or healthcare information tools.

We plan to extend this work in two different directions. We want to experiment with optimizing the location of Wi-Fi RTT beacons using our previously developed technique [15]. Generating a beacon map with optimized placement for best possible measurements will allow us to test the localization accuracy of our system with a less dense beacon map. Second, we plan to collect a large dataset to have more samples with different user behaviors.

8 Conflict of Interest

On behalf of all authors, the corresponding author states that there is no conflict of interest.

References

1. Adib, F., Kabelac, Z., Katabi, D.: Multi-person localization via rf body reflections. In: Proceedings of the 12th USENIX Conference on Networked Systems Design and Implementation, NSDI'15, pp. 279–292. USENIX Association (2015)
2. Arulampalam, M., Maskell, S., Gordon, N., Clapp, T.: A tutorial on particle filters for online nonlinear/non-gaussian bayesian tracking. Trans. Sig. Proc. **50**(2), 174–188 (2002). DOI 10.1109/78.978374
3. Azizyan, M., Constandache, I., Choudhury, R.R.: SurroundSense: Mobile Phone Localization Via Ambience Fingerprinting. International Conference on Mobile Computing and Networking (MobiCom'09) pp. 261–272 (2009). DOI 10.1145/1614320.1614350
4. Bao, X., Liu, B., Tang, B., Hu, B., Kong, D., Jin, H.: PinPlace: Associate Semantic Meanings with Indoor Locations Without Active Fingerprinting. International Joint Conference on Pervasive and Ubiquitous Computing (UbiComp'15) pp. 921–925 (2015). DOI 10.1145/2750858.2807543
5. Biehl, J.T., Cooper, M., Filby, G., Kratz, S.: LoCo: A Ready-to-Deploy Framework for Efficient Room Localization Using Wi-Fi. International Joint Conference on Pervasive and Ubiquitous Computing (UbiComp'14) pp. 183–187 (2014). DOI 10.1145/2632048.2636083
6. Biehl, J.T., Girgensohn, A., Patel, M.: Achieving accurate room-level indoor location estimation with emerging iot networks. In: International Conference on the Internet of Things (2019)
7. Biehl, J.T., Turner, T., van Melle, W., Girgensohn, A.: myunity: A new platform to support communication in the modern workplace. In: Proceedings of the 19th ACM international conference on Multimedia, pp. 801–802 (2011). DOI 10.1145/2072298.2072465
8. Cheng, Y.K., Chang, R.Y.: Device-Free Indoor People Counting Using Wi-Fi Channel State Information for Internet of Things. IEEE Global Communications Conference (GlobeCom'17) pp. 1–6 (2017). DOI 10.1109/glocom.2017.8254522
9. Cheng, Y.M.: Using ZigBee and Room-Based Location Technology to Constructing an Indoor Location-Based Service Platform. International Conference on Intelligent Information Hiding and Multimedia Signal Processing pp. 803–806 (2009). DOI 10.1109/iih-msp.2009.106
10. CompuLab WILD WiFi router supports WiFi RTT (802.11mc) location. CNXSOFT - Embedded Systems News (2018). URL `https://www.cnx-software.com/2018/09/05/compulab-wild-wifi-rtt-router-802-11mc/`
11. Constandache, I., Agarwal, S., Tashev, I., Choudhury, R.R.: Daredevil: Indoor Location Using Sound. ACM SIGMOBILE Mobile Computing and Communications Review **18**, 9–19 (2014). DOI 10.1145/2636242.2636245
12. Cooper, M., Biehl, J., Filby, G., Kratz, S.: LoCo: Boosting for Indoor Location Classification Combining Wi-Fi and BLE. Personal and Ubiquitous Computing **20**, 83–96 (2016). DOI 10.1007/s00779-015-0899-z
13. De Cillis, F., De Simio, F., Faramondi, L., Inderst, F., Pascucci, F., Setola, R.: Indoor positioning system using walking pattern classification. In: 22nd Mediterranean Conference on Control and Automation, pp. 511–516 (2014). DOI 10.1109/MED.2014.6961424
14. Evaluating AAL systems through competitive benchmarking. `http://evaal.aaloa.org/2016/competition-results`. Accessed: 2018-Feb-24
15. Falque, R., Patel, M., Biehl, J.: Optimizing placement and number of rf beacons to achieve better indoor localization. In: 2018 IEEE International Conference on Robotics and Automation (ICRA), pp. 2304–2311 (2018)
16. Hernández, N., Ocaña, M., Alonso, J.M., Kim, E.: Continuous Space Estimation: Increasing WiFi-Based Indoor Localization Resolution without Increasing the Site-Survey Effort. Sensors **17**, 147 (2017). DOI 10.3390/s17010147
17. Ibrahim, M., Liu, H., Jawahar, M., Nguyen, V., Gruteser, M., Howard, R., Yu, B., Bai, F.: Verification: Accuracy Evaluation of WiFi Fine Time Measurements on an Open Platform. Internation Conference on Mobile Computing and Networking (MobiCom'18) (2018). DOI 10.1145/3241539.3241555
18. IEEE Standard for Information technology — Telecommunications and information exchange between systems Local and metropolitan area networks — Specific requirements - Part 11: Wireless LAN Medium Access Control (MAC) and Physical Layer (PHY) Specifications. IEEE Std 802.11-2016 (Revision of IEEE Std 802.11-2012) pp. 1–3534 (2016). DOI 10.1109/ieeestd.2016.7786995
19. Iqbal, S., Iqbal, U., Hassan, S.A., Saleem, S.: Indoor motion classification using passive rf sensing incorporating deep learning. In: 2018 IEEE 87th Vehicular Technology Conference (VTC Spring), pp. 1–5 (2018)
20. Jadidi, M.G., Patel, M., Miró, J.V., Dissanayake, G., Biehl, J.T., Girgensohn, A.: A radio-inertial localization and tracking system with BLE beacons prior maps. In: 2018 International Conference on Indoor Positioning and Indoor Navigation, IPIN 2018, pp. 206–212 (2018)
21. Jaén, L., Álvare, F.J., Aguilera, T., García, J.J.: Room-level Indoor Positioning Based on Acoustic Impulse Response Identification. International Conference on Indoor Positioning and Indoor Navigation (IPIN'17) pp. 1–10 (2017)
22. Kohlbrecher, S., Meyer, J., von Stryk, O., Klingauf, U.: A flexible and scalable slam system with full 3d motion estimation. Proc. IEEE International Symposium on Safety, Security and Rescue Robotics (SSRR) (2011)
23. Kong, F., Chen, Y., Xie, J., Zhang, G., Zhou, Z.: Mobile robot localization based on extended kalman filter. World Congress on Intelligent Control and Automation **2**, 9242–9246 (2006). DOI 10.1109/WCICA.2006.1713789
24. Kyritsis, A.I., Kostopoulos, P., Deriaz, M., Konstantas, D.: A BLE-Based Probabilistic Room-Level Localization Method. Proceedings of the International Conference on Localization and GNSS (ICL-GNSS'16) pp. 1–6 (2016). DOI 10.1109/icl-gnss.2016.7533848
25. Lee, A.J., Biehl, J.T., Curry, C.: Sensing or Watching?: Balancing Utility and Privacy in Sensing Systems via Collection and Enforcement Mechanisms. Symposium on Access Control Models and Technologies (SACMAT'18) pp. 105–116 (2018). DOI 10.1145/3205977.3205983
26. Lee, S., Kim, Y., Ahn, D., Ha, R., Lee, K., Cha, H.: Non-obstructive Room-level Locating System in Home Environments Using Activity Fingerprints from Smartwatch. International Joint Conference on Pervasive and Ubiquitous Computing (UbiComp'15) pp. 939–950 (2015). DOI 10.1145/2750858.2804272
27. Liu, K., Liu, X., Li, X.: Guoguo: Enabling Fine-Grained Smartphone Localization via Acoustic Anchors. IEEE Transactions on Mobile Computing **15**, 1144–1156 (2015). DOI 10.1109/tmc.2015.2451628
28. Lupton, T., Sukkarieh, S.: Visual-inertial-aided navigation for high-dynamic motion in built environments without initial conditions. IEEE Transactions on Robotics **28**(1), 61–76 (2012)

29. Ma, S., Liu, Q., Kim, C., Sheu, P.: Lift: Using Projected Coded Light for Finger Tracking and Device Augmentation. IEEE International Conference on Pervasive Computing and Communications (PerCom'17) pp. 153–159 (2017). DOI 10.1109/percom.2017.7917861
30. Nagpal, P.S., Rashidzadeh, R.: Indoor Positioning using Magnetic Compass and Accelerometer of Smartphones. International Conference on Selected Topics in Mobile and Wireless Networking (MoWNeT'13) pp. 140–145 (2013). DOI 10.1109/mownet.2013.6613810
31. Patel, M., Girgensohn, A., Biehl, J.: Fusing Map Information with a Probabilistic Sensor Model for Indoor Localization Using RF Beacons. International Conference on Indoor Positioning and Indoor Navigation (IPIN'18) pp. 1–8 (2018). DOI 10.1109/IPIN.2018.8533758
32. Patel, S.N., Truong, K.N., Abowd, G.D.: PowerLine Positioning: A Practical Sub-room-level Indoor Location System for Domestic Use. International Conference on Ubiquitous Computing (UbiComp'06) pp. 441–458 (2006). DOI 10.1007/11853565_26
33. Pei, L., Liu, J., Guinness, R., Chen, Y., Kuusniemi, H., Chen, R.: Using ls-svm based motion recognition for smartphone indoor wireless positioning. Sensors **12**(5), 6155–6175 (2012). DOI 10.3390/s120506155
34. Quigley, M., Conley, K., Gerkey, B., Faust, J., Foote, T., Leibs, J., Wheeler, R., Ng, A.Y.: ROS: an Open-Source Robot Operating System. ICRA workshop on open source software **3**(3.2), 5 (2009)
35. Rossi, M., Seiter, J., Amft, O., Buchmeier, S., Tröster, G.: RoomSense: an Indoor Positioning System for Smartphones Using Active Sound Probing. Augmented Human International Conference (AH'13) pp. 89–95 (2013). DOI 10.1145/2459236.2459252
36. Shang, J., Gu, F., Hu, X., Kealy, A.: APFiLoc: An Infrastructure-Free Indoor Localization Method Fusing Smartphone Inertial Sensors, Landmarks and Map Information. Sensors **15**, 27251–27272 (2015). DOI 10.3390/s151027251
37. Silva, P.F., Lohan, E.S.: Room-level Indoor Positioning with Wi-Fi and RFID fingerprints. International Workshop on Mobile Entity Localization and Tracking in GPS-less Environments pp. 5:1–5:2 (2015). DOI 10.1145/2830571.2830579
38. Song, H., Choi, W., Kim, H.: Robust vision-based relative-localization approach using an rgb-depth camera and lidar sensor fusion. IEEE Transactions on Industrial Electronics **63**(6), 3725–3736 (2016). DOI 10.1109/TIE.2016.2521346
39. Tachikawa, M., Maekawa, T., Matsushita, Y.: Predicting Location Semantics Combining Active and Passive Sensing with Environment-independent Classifier. International Joint Conference on Pervasive and Ubiquitous Computing (UbiComp'16) pp. 220–231 (2016). DOI 10.1145/2971648.2971684
40. Thrun, S.: Particle filters in robotics. Conference on Uncertainty in Artificial Intelligence pp. 511–518 (2002)
41. Thrun, S., Burgard, W., Fox, D.: Probabilistic Robotics (Intelligent Robotics and Autonomous Agents series). Intelligent Robotics and Autonomous Agents. The MIT Press (2005)
42. Wang, S., Clark, R., Wen, H., Trigoni, N.: End-to-end, sequence-to-sequence probabilistic visual odometry through deep neural networks. The International Journal of Robotics Research **37**(4-5), 513–542 (2018). DOI 10.1177/0278364917734298
43. Want, R., Hopper, A., Falcão, V., Gibbons, J.: The active badge location system. ACM Transactions on Information Systems (TOIS) **10**, 91–102 (1992). DOI 10.1145/128756.128759
44. Want, R., Wang, W., Chesnutt, S.: Accurate Indoor Location for the IoT. Computer **51**, 66–70 (2018). DOI 10.1109/mc.2018.3191259
45. Wilson, J., Patwari, N.: See-Through Walls: Motion Tracking Using Variance-Based Radio Tomography Networks. IEEE Transactions on Mobile Computing **10**, 612–621 (2010). DOI 10.1109/tmc.2010.175
46. Xu, Q., Zheng, R., Hranilovic, S.: Idyll: Indoor localization using inertial and light sensors on smartphones. In: Proceedings of the 2015 ACM International Joint Conference on Pervasive and Ubiquitous Computing, UbiComp '15, pp. 307–318. ACM (2015). DOI 10.1145/2750858.2807540
47. Yoon, P.K., Zihajehzadeh, S., Kang, B., Park, E.J.: Adaptive Kalman Filter for Indoor Localization using Bluetooth Low Energy and Inertial Measurement Unit. International Conference of the IEEE Engineering in Medicine and Biology Society (EMBC'15) pp. 825–828 (2015). DOI 10.1109/EMBC.2015.7318489
48. Zhang, C., Zhang, X.: Pulsar: Towards Ubiquitous Visible Light Localization. International Conference on Mobile Computing and Networking (MobiCom'17) pp. 208–221 (2017). DOI 10.1145/3117811.3117821
49. Zhou, Z., Zhang, J., Zhang, Y.D.: Ultra-wideband radar and vision based human motion classification for assisted living. In: 2016 IEEE Sensor Array and Multichannel Signal Processing Workshop (SAM), pp. 1–5 (2016). DOI 10.1109/SAM.2016.7569747